THE METEOROLOGICAL MAGAZINE

October 1987

Met.O.978 No. 1383 Vol. 116

METEOROLOGICAL OFFICE Met.O.978

THE METEOROLOGICAL MAGAZINE

No. 1383, October 1987, Vol. 116

551.515.827(261.26)

Case study of a persistent mesoscale cold pool

F.F. Hill*

Meteorological Office, Bracknell

K.A. Browning

Deputy Director (Physical Research), Meteorological Office, Bracknell

Summary

A case study is presented of a shallow mesoscale cold pool of diameter 500 km which formed near the southern end of a disrupting upper trough. The cold pool remained within the circulation of a blocking high and survived with a steady-state thickness anomaly for 5 days. During this time it moved first eastwards across southern Britain and then westwards across northern France and the English Channel. Thundery rain occurred close to the centre during its return journey. The cold pool was not easily identifiable on conventional 1000–500 mb thickness charts but was well revealed by analyses of 700–500 mb thickness and, even better, by analyses of isentropic potential vorticity (IPV). A well-defined region of high IPV was associated with subsided stratospheric air immediately above the cold pool and it advected like a passive tracer. During their eastward journey, the cold pool and IPV maximum were associated with a well-marked open wave which, because of the limited extent of cloud, was best revealed by Meteosat water vapour imagery. During the subsequent westward journey, the position of the cold pool was indicated in Meteosat water vapour imagery by an eye-catching swirl of dry air surrounding a moist core.

1. Introduction

Cold pools, otherwise referred to as upper cold lows, cut-off lows, cold-core cyclones, cold vortices or cold domes, have been the subject of study for many years. Early analytical studies by Palmen (1949) and others showed that they form from the cutting off of a pocket of polar air near the southern extremity of a cold trough. Such systems can be over 1000 km in diameter and can last for many days (e.g. Peltonen 1963). Recent studies (e.g. Matsumoto *et al.* 1982) show that they can also occur on the mesoscale when, despite their small size, they give rise to significant precipitation systems. A feature of cold pools discussed by Palmen is the existence of a warm core above them. Matsumoto and Ninomiya (1967) point out that a warm core at tropopause level can provide a good indication of the existence of even a very small cold pool within the troposphere.

Potential vorticity is a particularly useful diagnostic quantity not least because it is often, to a good approximation, advected as a passive tracer along surfaces of constant potential temperature. Potential vorticity is the product of the absolute vorticity and the static stability and, when calculated along isentropic surfaces, is abbreviated to IPV.

* Now at Royal Air Force, High Wycombe.

High values of IPV have been revealed along surfaces which intersect the warm core above a cold pool, implying that this air had descended from the lower stratosphere where such values are commonplace (Eliassen and Kleinschmidt 1957, Degorska 1980). The stratospheric origin of the air in such regions was indicated in studies of tropopause folding by Danielsen (1968) and Danielsen and Mohnen (1977). More recently Hoskins *et al.* (1985), in discussing the general versatility of IPV maps, have suggested that, whereas the low temperature-anomaly of a cold pool may well be important from a purely diagnostic point of view, it can be argued that in terms of cause and effect its importance is secondary by comparison with that of the IPV advection above it. This is because much of the coldness of a cold pool is attributable to the induced temperature field of the IPV maximum above it.

Sumner (1953) carried out a statistical study of cold pools in an area of particular interest to UK forecasters, south of 80° N between 60° W and 30° E. He found that cold pools having at least two closed 1000–500 mb thickness contours (contours drawn at 60 m intervals) persisted on average for 3 days, with no clear relation between the intensity of the cold pool and its duration. Many cold pools were found to occur in association with surface anticyclones and these were found to be accompanied by what was regarded as a surprisingly high occurrence of precipitation.

The purpose of the present paper is to show by means of a case study, using output from the Meteorological Office fine-mesh model together with satellite imagery, that a seemingly anomalous patch of convective showers and thunderstorms within the circulation of an anticyclone was associated with a long-lived mesoscale feature that was manifested in the middle troposphere as a cold pool, and in the upper troposphere and lower stratosphere as a warm region with a pronounced maximum of IPV. The cold pool was a minor feature in conventional 1000–500 mb thickness analyses because the thickness anomaly was small and restricted to a shallow layer. The overall phenomenon, however, of which the thickness anomaly was a part, was more significant when viewed in terms of the IPV anomaly aloft and this feature has been used to backtrack to find the origin of the cold pool before it reached the data-dense region of north-west Europe. At times the influence of the mesoscale feature could be seen to extend over a rather large area when viewed by satellite in terms of the distortion of the upper-tropospheric humidity field.

2. Synoptic setting

The synoptic setting for this event is shown in Figs 1 and 2 which illustrate the situation about half-way through the life cycle of the mesoscale cold pool. Fig. 1 shows the surface analysis and Fig. 2 the 500 mb and 1000–500 mb thickness analyses at 00 GMT on 24 April 1984. The cold pool can just be discerned in the thickness analysis over the English Channel on the southern flank of the anticyclone. The corresponding infra-red imagery from Meteosat (not shown) revealed an isolated patch of cold convective cloud tops associated with the cold pool. Water vapour imagery from Meteosat (Fig. 3) showed a swirl of dry upper-tropospheric air around the moist core associated with the convection at the centre of the cold pool. This swirl in the moisture distribution persisted as an eye-catching feature of the satellite water vapour imagery for the next 2 days and it was this that drew attention to the possibility that, despite the bland appearance of the routine synoptic analyses, the patch of showers at its focus might be other than just a random and inherently unpredictable event.

3. Persistence and movement of the cold pool and associated IPV anomaly

Fig. 4 shows part of the life history of the cold pool by means of a sequence of four analyses of the 700–500 mb layer at 24-hour intervals using a contour interval of 20 m. This layer was chosen rather than the more usual 1000–500 mb because no temperature anomaly could be detected below 700 mb. There are sufficient radiosonde measurements to enable a cold pool to be revealed with closed contours

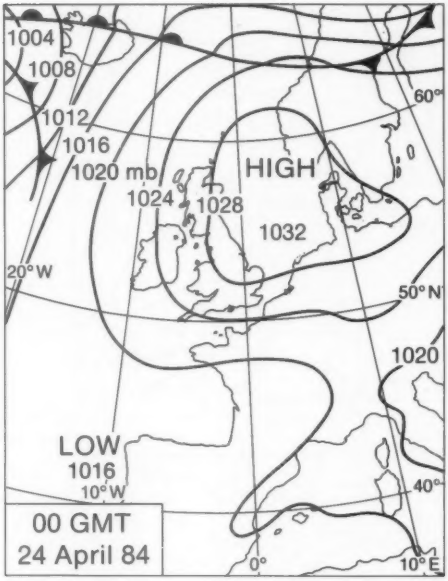

Figure 1. Surface analysis for 00 GMT on 24 April 1984.

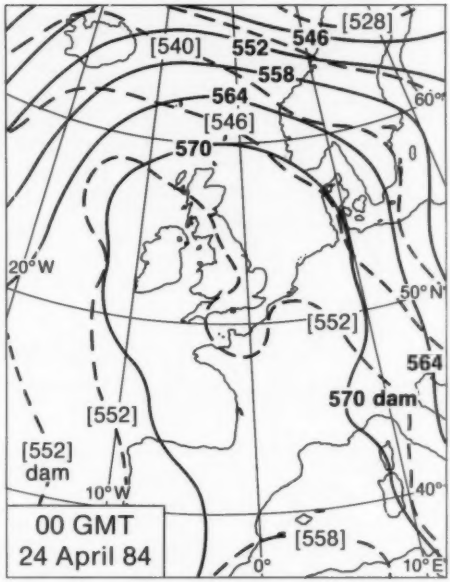

Figure 2. 500 mb contour (solid lines) and 1000–500 mb thickness (dashed lines) analyses for 00 GMT on 24 April 1984.

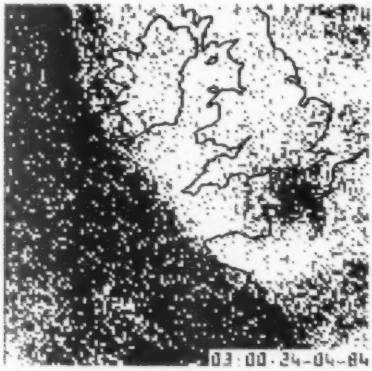

Figure 3. Meteosat water vapour imagery for 03 GMT on 24 April 1984. Areas of high and low humidity in the upper troposphere are shown black and white, respectively. The speckled effect is due to instrumental noise.

throughout the period from 00 GMT on the 22nd to 12 GMT on the 25th and to suggest that the central thickness was close to about 2560 m. For most of the time during which it was well observed, the cold pool remained almost constant in size and depth. The circulation in the 700–500 mb thermal winds extended to 500 km in diameter, although the thickness anomaly was only about 50 m. Because of the smallness of this thickness anomaly, the cold pool was sometimes difficult to identify in UK operational

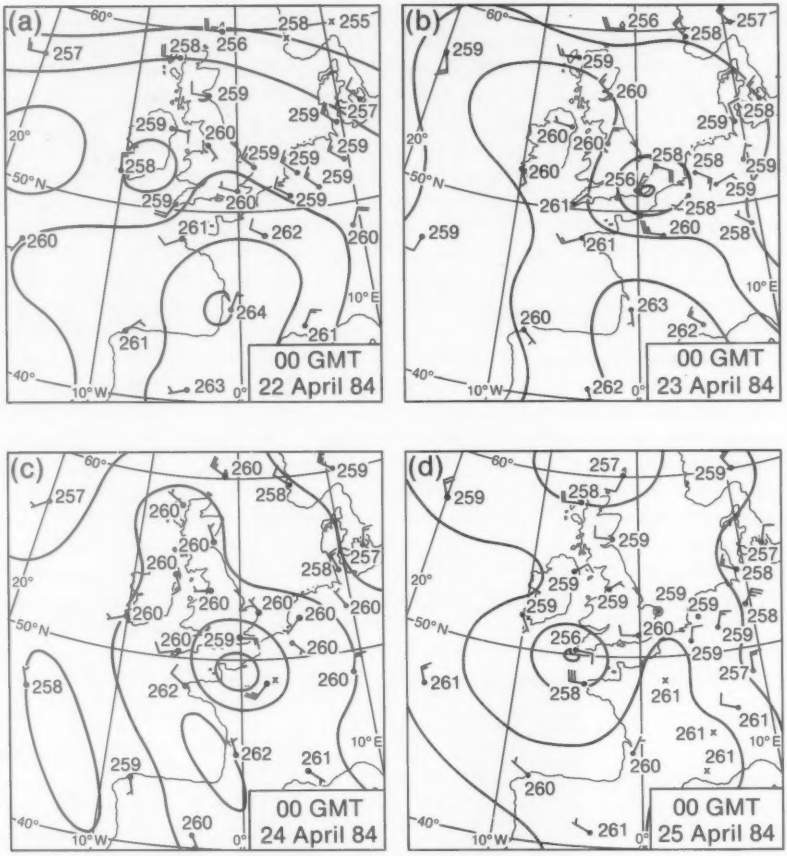

Figure 4. 700–500 mb thickness analyses showing the location of the cold pool at 00 GMT on (a) 22 April, (b) 23 April, (c) 24 April and (d) 25 April 1984. Thickness contours are at 2 dam intervals. Thermal winds and thickness values (dam) are shown for individual radiosonde stations.

thickness charts in which the contours are conventionally drawn at 60 m intervals, although it appears in the 1000–500 mb thickness analyses published by Deutscher Wetterdienst in the *European Meteorological Bulletin* for which the contour interval is 40 m.

The relationship and movement of the cold pool with respect to the 500 mb upper-air pattern is illustrated in Fig. 5. The cold pool, initially on the northern flank of a 500 mb ridge, moved east-north-eastwards towards southern Ireland. The ridge then intensified over Scotland and this caused the upper winds in the vicinity of the cold pool to weaken and veer, resulting in a more south-easterly movement of the cold pool towards northern France. By the morning of 24 April, the upper ridge had become firmly established as a blocking high over Scotland and the North Sea; the cold pool then travelled in a westerly direction around the southern flank of the block. After moving slowly along the English Channel, it

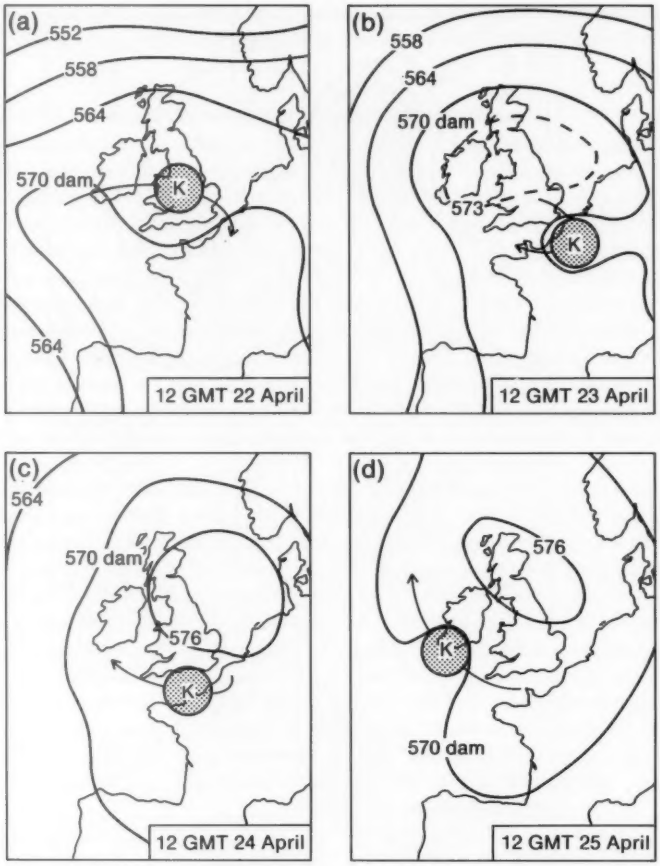

Figure 5. Position (K) of the centre of the cold pool (stippled area), from the 700–500 mb thickness contours of Fig. 4, plotted in relation to the 500 mb contours at 12 GMT on (a) 22 April, (b) 23 April, (c) 24 April and (d) 25 April 1984. Arrows show the movement of the cold pool from H−24 to H+24 in each case.

accelerated as it turned north-westwards towards Ireland. The cold pool probably decayed when it was some 300 km to the north-west of Ireland, early on 26 April.

A well-defined IPV maximum was located above the cold pool throughout its existence. Fig. 6 shows a sequence of nine IPV charts at 12-hour intervals for the 330 K isentropic surface, situated between 250 and 200 mb. These have been calculated using analyses from the Meteorological Office fine-mesh model, the resolution of which is 0.75° latitude by 0.94° longitude. It can be seen from Fig. 6 that the core of high IPV within the 330 K isentropic surface associated with the cold pool was identified fairly consistently in size and intensity from one analysis to the next from 00 GMT on the 22nd until 00 GMT on the 25th. (Before the start of this period it was part of a band of high IPV associated with an upper trough (see section 5), and at the end of this period it merged with the large region of high IPV to the west

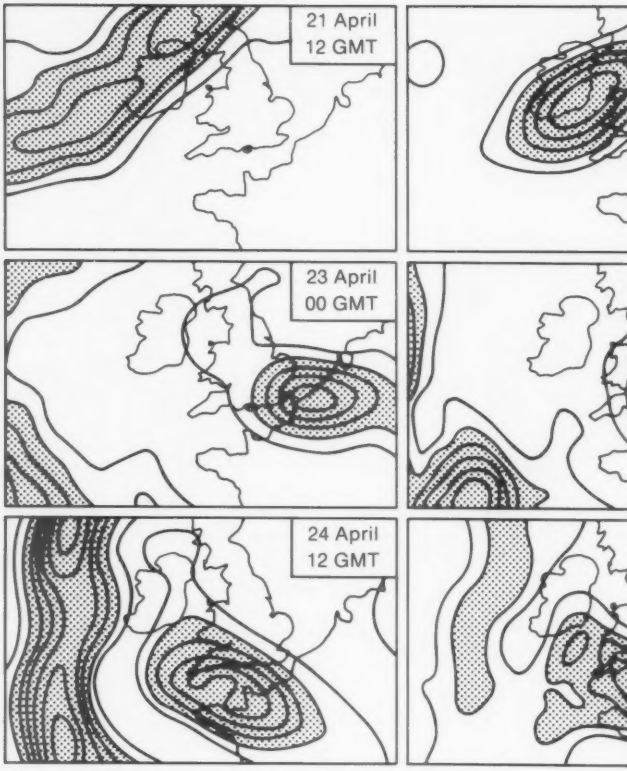

Figure 6. IPV on the 330 K isentropic surface at 12-hour intervals starting at 12 GMT
units of 10^{-6}m^{2}K kg^{-1}s^{-1} as suggested by Hoskins *et al.* (1985), where one of these uni
and there is a vertical gradient in θ of 1 K per 10 mb. According to Hoskins *et al.* (198
air.

MT on 21 April 1984. Contours are drawn at intervals of 1 IPV unit corresponding to units is equivalent to a relative vorticity of zero when the Coriolis parameter is $10^{-4}s^{-1}$ 1985), a value of 2 or more IPV units (shaded regions) is characteristic of stratospheric

of Ireland.) A comparison of Figs 5 and 6 confirms that, as is to be expected, the centre of the region of high IPV moved along a path which coincided with that of the cold pool, effectively acting as a passive tracer.

4. The relationship of the mesoscale cold pool and the IPV maximum

A comparison is made in Fig. 7 between IPV analyses from the Meteorological Office fine-mesh model in the 330 K and the 310 K isentropic surfaces; both IPV values and the pressure height of the isentropic surfaces are shown. The 330 K surface was located just below the tropopause as defined by the lapse rate, whereas the 310 K surface intersected the upper part of the cold pool well within the troposphere. It can be seen that the large IPV values in the 330 K surface did not extend down into the 310 K surface. However, the pressure-height minimum in the 310 K surface, which identifies the centre of the cold pool, was located directly beneath the IPV maximum in the 330 K surface. The diagnostic necessity of a close structural linkage between the cold pool and the overlying IPV maximum is well known (Hoskins *et al.* 1985). The vertical structure as derived from the fine-mesh model is clearly revealed by the cross-section in Fig. 8. The cold pool is identified by the dashed envelope within which the isentropes locally bulge upwards, and the top of the cold pool is at about 330 mb. The IPV maximum, centred near 240 mb, extends down into the middle troposphere and intersects the top of the cold pool.

The effect of the passage of the cold pool on the temperature distribution aloft is clearly brought out by the ascents at two radiosonde stations in southern England (Fig. 9). The cold pool passed south-eastwards across Crawley just before the time of the 00 GMT ascent on 23 April and was approaching Camborne at the time of the 00 GMT ascent on 25 April. Comparing each of these ascents (solid lines in Fig. 9) with corresponding ascents obtained 12 hours earlier (dashed lines in Fig. 9), it can be seen that the air became potentially unstable within the cold pool from 850 to 430 mb as the result of a temperature decrease of around 4 °C in the middle troposphere; at the same time, the air warmed by nearly 5 °C between 400 and 200 mb. Since IPV values exceeding 2 are likely to be associated with stratospheric air, we can deduce from Figs 6 to 9 that the upper tropospheric warming above the cold pool was due to adiabatic warming caused by the descent of air of stratospheric origin. Moreover, according to Hoskins *et al.* (1985) the overrunning high-IPV air probably induced ascent beneath it and this led to the adiabatic cooling that sustained the cold pool in the middle levels.

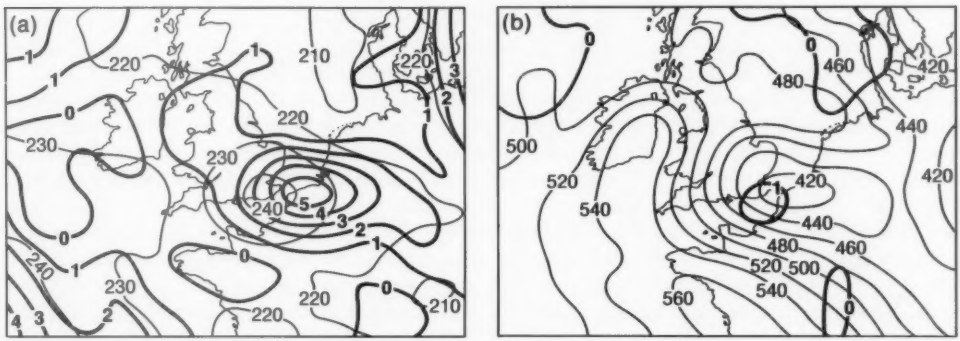

Figure 7. IPV (bold contours labelled in IPV units) and pressure level (fine contours labelled in millibars) of the corresponding isentropic surface at 00 GMT on 23 April 1984 for (a) the 330 K surface and (b) the 310 K surface.

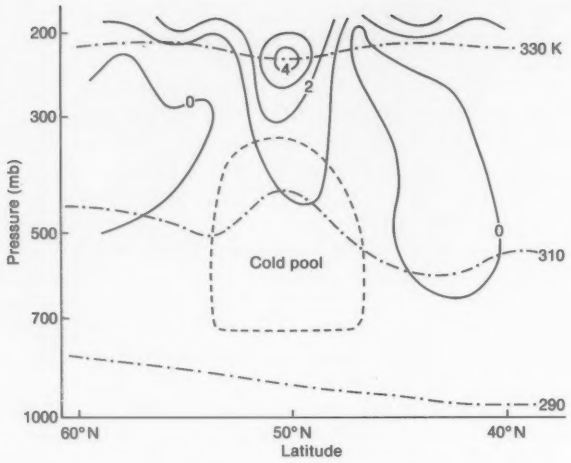

Figure 8. North–south cross-section at 1 °E through the cold pool at 00 GMT on 23 April 1984 when it was near south-east England. Bold contours show IPV in IPV units. Undulating dash-dot lines show isentropic surfaces. The dashed line outlines the cold pool.

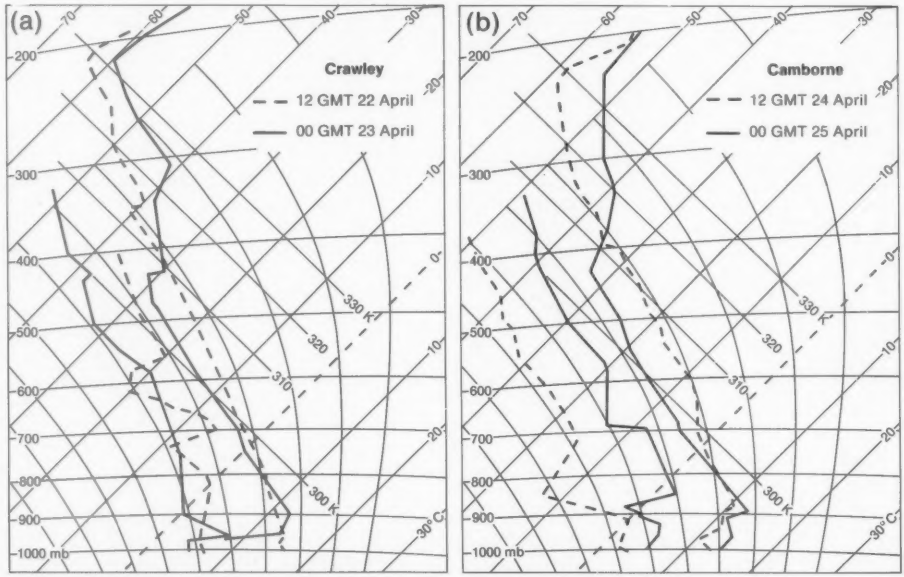

Figure 9. Tephigrams showing radiosonde ascents at (a) Crawley and (b) Camborne close to the centre of the cold pool as it passed overhead (continuous lines) compared with the ascents made at the corresponding stations 12 hours earlier (dashed lines).

5. Initial development of the cold pool

The cold pool developed within a region of high pressure south-west of Ireland on or before 21 April. Because of the dearth of radiosonde stations in this region it was not revealed clearly in the thickness analyses. However, its existence could be inferred from IPV analyses and it was also associated with a characteristic pattern in the satellite imagery, especially the water vapour imagery.

Earlier IPV analyses on 19 April had shown a broad band of high IPV on the 330 K surface extending from south-west to north-east across the Atlantic to the north of the surface fronts. As the upper trough sharpened behind the cold front, so the zone of high IPV extended southwards to 45° N. The forward edge of this zone caught up with the surface cold front during 20 April (Fig. 10(a)). Although the highest values of IPV were associated with the north-eastward-moving depression, a secondary maximum was cut off near 51° N, 30° W between 00 and 12 GMT on 20 April and it moved eastwards towards southern Ireland by 00 GMT on the 22nd (Fig. 10(b)). It is not known from the available data whether the cold pool itself existed on 20 April or developed during the next 24 hours, but it is clear from satellite imagery that the increased cyclonic vorticity in this region had already induced a small wave in the upper cloud at the rear of the cold front early in the morning of 21 April.

By 03 GMT on 22 April the wave was very clearly defined in the infra-red imagery and even more so in the water vapour imagery (Fig. 11(a)). The solid black area over England and Wales in Fig. 11(a) corresponds to upper cloud; the speckled band extending westwards from the wave corresponds to a band of moist upper-tropospheric air which was not producing cloud. The arrow shows the centre of the cold pool. Patches of moist air were found near the centre of the cold pool but much drier upper-tropospheric air (white area in Fig. 11(a)) can be seen around the southern flank of the cold pool. The dry air was associated with the veered flow to the rear of the upper trough (see the wind arrows over south-west Ireland in Fig. 10(b)). As shown in Figs 11(b) and (c), this dry air spread rapidly across southern England and the English Channel as the wave developed. It is this dry air that could be seen swirling around the cold pool during the ensuing days and which led to the eye-catching water vapour image in Fig. 3.

6. Weather associated with the cold pool

The cloud and precipitation associated with the cold pool varied a lot during the 5 days of its existence. Ascent at upper levels ahead of the eastward-moving cold pool caused a broad band of cirrostratus and altostratus to move across southern Ireland on 21 April. This cloud covered most of England and Wales during the night of 21/22 April and had the shape of an open wave in both the infra-red and water vapour imagery (Fig. 11(a)). However, very little rain reached the ground from this extensive area of mainly middle- and upper-level cloud which dispersed as it moved east-north-eastwards during 22 April. Near the centre of the cold pool, bands of altocumulus castellanus gave intermittent rain over central southern England during the afternoon of 22 April. These bands crossed south-east England and dispersed overnight, and by the morning of 23 April, just before the cold pool started returning westwards, there was no cloud near the cold pool.

When the cold pool was returning westwards, areas of thundery rain or showers developed intermittently within it. The location and size of the main areas of convective cloud are illustrated in Fig. 12. A substantial proportion of these areas was occupied by thundery rain which was locally heavy. It can be seen that all the cloud formed within the cold pool as outlined by the 2580 m contour in the 700–500 mb thickness charts. Most of the vigorous convective cloud formed close to the central moist core, while more patchy cloud moved cyclonically around it.

It is apparent from Fig. 9 that air temperatures near the ground of at least 20 °C were required for convection to be initiated by surface heating. Such temperatures were exceeded over northern France

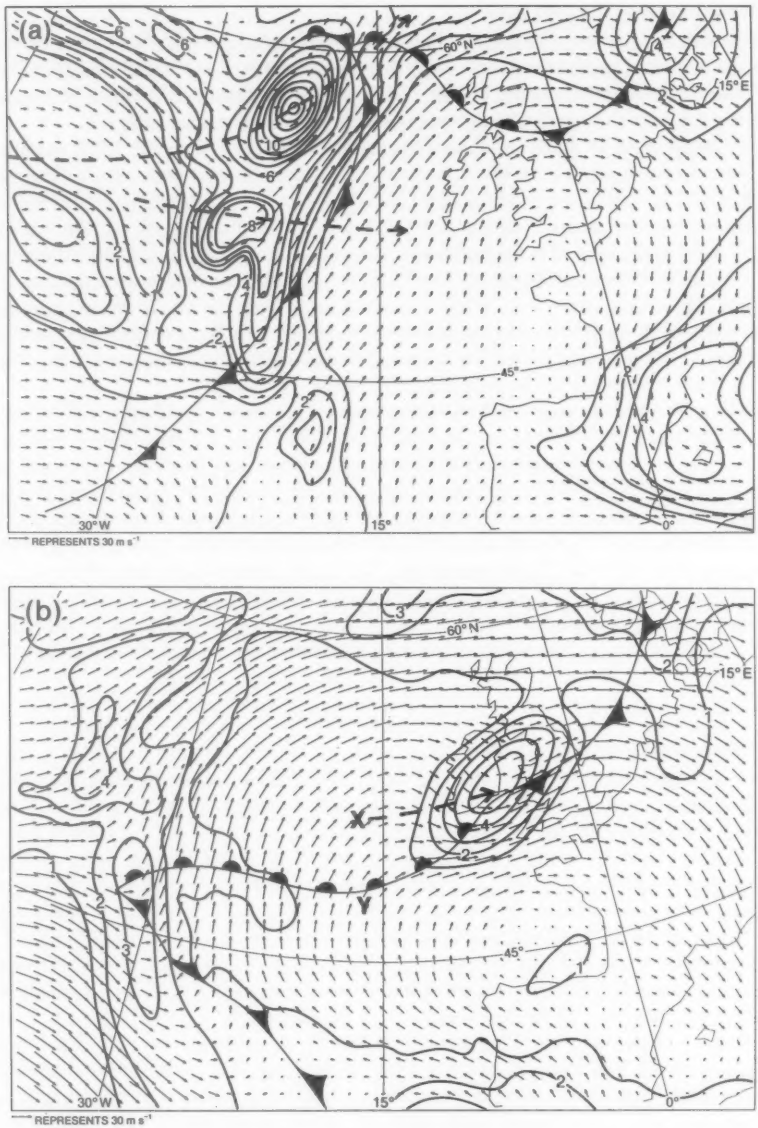

Figure 10. IPV (in IPV units) and flow in the 330 K surface at (a) 12 GMT on 20 April and (b) 00 GMT on 22 April 1984, with surface fronts superimposed. Bold dashed arrows show the direction of travel of the main and secondary IPV maxima. The cold pool was associated with the secondary IPV maximum which travelled in an almost easterly direction from X in (b). 18 hours earlier when the IPV maximum was at X the cold front wave was located to the south of it at Y.

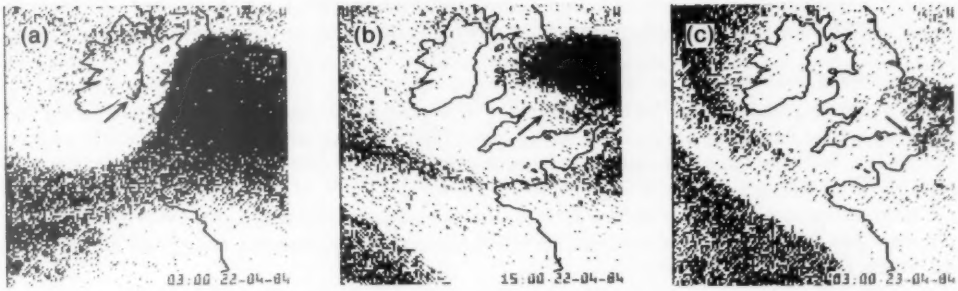

Figure 11. Meteosat water vapour imagery for (a) 03 GMT on 22 April, (b) 15 GMT on 22 April and (c) 03 GMT on 23 April 1984. Areas of high and low humidity in the upper troposphere are shown black and white, respectively, as in Fig. 3. The arrows point to the centre of the 700–500 mb cold pool.

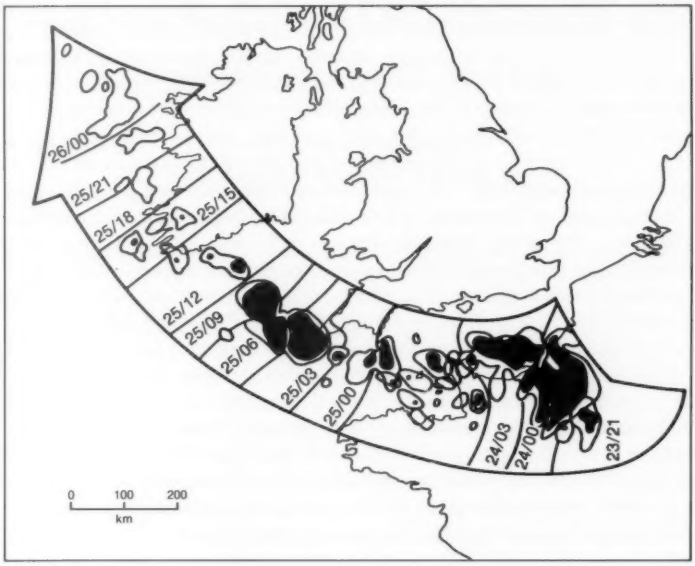

Figure 12. Locations of cumulonimbus (black) and thick altocumulus clouds (outlines) at 3-hour intervals during the period from 21 GMT on 23 April to 00 GMT on 26 April 1984 as inferred mainly from satellite imagery. These convective clouds were closely associated with the centre of the cold pool, whose path is shown by the broad arrow.

during the afternoon of 23 April prior to the development of the storms there. Another warm day occurred on 24 April near the north coast of France; this almost certainly accounts for the small thundery areas which formed briefly to the west of the Cherbourg peninsula early that afternoon. On the other hand, it is clear from the Camborne ascent in Fig. 9(b) that the development, during the night of 24/25 April, of the storm area near Cornwall was not due to local surface heating, since surface air temperatures over the English Channel were only 12 °C. The Camborne ascent shows that there was a

layer of potentially unstable warm moist air centred at 850 mb which was enabling the convection to be sustained. This warm moist air appeared to have originated from near the surface over northern France.

7. Concluding remarks

An underlying message of this study is that a mesoscale event can have more organization and persistence than might reasonably have been expected. By carrying out a detailed case study we have obtained a clear description of a non-severe mesoscale event, and determined what kinds of data are suitable for revealing it.

The mesoscale cold pool that we have studied had a circulation extending to 500 km in diameter and, although poorly revealed in conventional 1000–500 mb analyses, its presence was clearly identified by the following three kinds of data:

(a) 700–500 mb thickness, the maximum thickness anomaly in the cold pool being 50 m.

(b) IPV in the 330 K isentropic surface, with a maximum value of typically $8 \times 10^{-6} m^2 K\ kg^{-1} s^{-1}$ occurring directly above the cold pool; the IPV tended to advect like a passive tracer and has been used to backtrack and locate the origin of the cold pool.

(c) Water vapour imagery, with eye-catching patterns that revealed a mass of dry middle- and upper-tropospheric air which invaded and eventually surrounded much of the cold pool.

The cold pool originated within cold air from an upstream trough; the enhanced cooling within the cold pool was consistent with adiabatic cooling owing to local ascent induced when descending stratospheric air with high IPV overran it.

The weather associated with the cold pool in this case study was easy to identify and track because it occurred within a region otherwise dominated by an anticyclone. Thus the cloud and precipitation for the most part was isolated and distinct. The cold pool itself began life as a remnant of an upper trough. Early in its life the cold pool was associated with a well-marked open wave in the satellite infra-red and water vapour imagery. The cloud produced by the wave was limited to the middle and upper troposphere, however, and little precipitation reached the ground. Subsequently this cloud dissipated altogether and a compact area of showers and thunderstorms formed near its centre in association with convection from the surface. Normally the warming due to such convection more than compensates for the combined cooling, due to large-scale adiabatic ascent and long-wave radiation, leading to the demise of a cold pool. However, this cold pool lasted 5 days with a constant thickness anomaly of 50 m. The longevity in this case was perhaps due in part to the limited extent and vigour of the convection because of its location within a region of dry air associated with the surrounding large-scale subsidence. Sumner (1953) in his study of over 200 cold pools found an average diurnal variation of about 20 m in central thickness which he attributed to insolation and the associated convection. In the present study no diurnal variation in thickness could be discerned and this is consistent with the rather limited amount of convection and the lack of diurnal variation in convective activity.

References

Danielsen, E.F. 1968 Stratospheric–tropospheric exchange based on radioactivity, ozone and potential vorticity. *J Atmos Sci*, **25**, 502–518.

Danielsen, E.F. and Mohnen, V.A. 1977 Project Duststorm Report: Ozone transport, in situ measurements and meteorological analyses of tropopause folding. *J Geophys Res*, **82**, 5867–5877.

Degorska, M. 1980 A case study of an upper cut-off cyclone development. *Publ Inst Geophys Pol Acad Sci*, **D-11(141)**, 111–123.

Eliassen, A. and Kleinschmidt, E. 1957 Dynamic meteorology. *In* Bartels, J. (ed.); Handbuch der Physik, Vol. 48. Berlin, Springer-Verlag.

Hoskins, B.J., McIntyre, M.E. and Robertson, A.W. 1985 On the use and significance of isentropic potential vorticity maps. *Q J R Meteorol Soc*, **111**, 877–946.

Matsumoto, S. and Ninomiya, K.	1967	On the mesoscale warm core above the condensation level related to convective activities under the influence of dome shaped cold air. *J Meteorol Soc Jpn*, **45**, 306–314.
Matsumoto, S., Ninomiya, K., Hasagawa, R. and Miki, Y.	1982	The structure and the role of a subsynoptic-scale cold vortex on the heavy precipitation. *J Meteorol Soc Jpn*, **60**, 339–354.
Palmen, E.	1949	Origin and structure of high-level cyclones south of the maximum westerlies. *Tellus*, **1**, 22–31.
Peltonen, T.	1963	A case study of an intense upper cyclone over eastern and northern Europe in November 1959. *Geophysica (Finland)*, **8**, 225–251.
Sumner, E.J.	1953	Cold pools: a statistical and synoptic study. *Meteorol Mag*, **82**, 291–301.

551.553.21:551.577.32(54):551.578.46

Variations in the onset of the summer monsoon over India

I. Subbaramayya and O.S.R.U. Bhanu Kumar

Department of Meteorology and Oceanography, Andhra University, Waltair, India

S. Vivekanandababu

Indian Institute of Technology, New Delhi, India

Summary

The dates of onset of the summer monsoon over India are quite variable. The trend and quasi-periodicity in the onset dates in the years 1956 to 1983 have been investigated. They indicate that the onset date is tending to become delayed all over India and that there are some significant periodic variations in different parts of the country. Increasing trends in the Himalayan, Eurasian and northern hemispheric snow covers and some significant periodic variations in the snow covers have also been found. The onset dates, particularly over Central India, are found to have a positive correlation with the snow cover.

1. Introduction

The start of the summer rains in India, which is known as the onset of the monsoon, is first apparent over the Andaman Islands (commonly called the Bay Islands) in the Bay of Bengal and gradually advances north-westwards. There have been many studies of the normal dates of onset, their variability, the associated upper-air circulation changes and how to forecast them (Maung Tun Yin 1949, Koteswaram 1958, Flohn 1964, Ramamurthi and Keshavamurty 1964, De la Mothe and Wright 1969, Ananthakrishnan 1970, Subbaramayya and Bhanu Kumar 1978, Kung and Sharif 1981). Of particular interest is the pulsatory nature of the advance of the monsoon reported by Subbaramayya *et al.* (1984). South peninsula is covered in one pulse, while north peninsula and parts of central India are covered in the second pulse. In another pulse the monsoon advances westward over a major part of north India (Fig. 1(a)). Considerable variability in the onset dates (Fig. 1(b)) was also found. In this paper the trend and quasi-periodicity of the variability is further examined.

2. Data and analysis

The Indian subcontinent was divided into six regions: south peninsula, north peninsula, north-east India, central north India, north-west India and west central India. These regions were chosen because in each of them the monsoon usually advances in one pulse (see Fig. 1(a)). Five or six stations in each

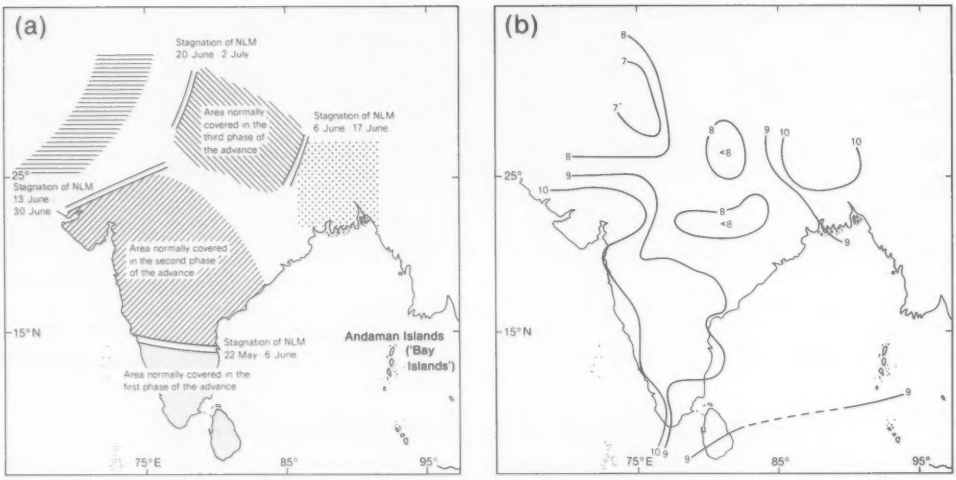

Figure 1. (a) Areas affected and periods of different phases in the advance of the monsoon, and (b) the variability of onset expressed as the standard deviation of the dates of onset. NLM is the northern limit of the monsoon.

region were selected, and the dates of onset at these stations in every year were determined from the northern limit of the monsoon, prepared for every day during the period of advance of the monsoon, for 28 years from 1956 to 1983. This follows the procedure described by Subbaramayya and Bhanu Kumar (1978). The regional averages were then obtained and analysed in the following way:

(a) The trend in the date of monsoon onset for each region was obtained by linear regression. The statistical significance of the trends was determined by Student's *t*-test.

(b) With the trend eliminated, the mean onset dates of each region were subjected to power spectrum analysis following the method described by Maruyama (1968). Power spectra were evaluated using different maximum lags to check the positions of power peaks. Consistent power peaks appeared in all cases; the spectra corresponding to a 16-year maximum lag are presented in this paper. The significance of the power peaks was assessed by the method given by Mitchell *et al.* (1966).

(c) Satellite derived monthly mean snow-cover data over the Himalayas (25–35° N and 60–105° E), Eurasia (5° S–70° N and 10° W–170° E) and the northern hemisphere for the years 1967–80 were obtained from NOAA-NESS. Though the length of the data is short, an attempt was made to examine whether there is any quasi-periodicity besides the trend.

(d) Correlations between monthly mean snow covers over the above three areas in February to May and the onset dates at selected stations were also calculated.

3. Results and discussion

3.1 *Onset dates*

The time series of onset dates for the six regions and the corresponding linear regression equations are presented in Fig. 2. In all six regions there is an increasing trend which means that the onset is getting later each year. The rate of change of onset date in south and north peninsula and north-east and west central India is 5–6 days per decade, while in central north India it is 3.5 days per decade and only 1 day per decade in north-west India. These trends could be only temporary and it cannot be expected that

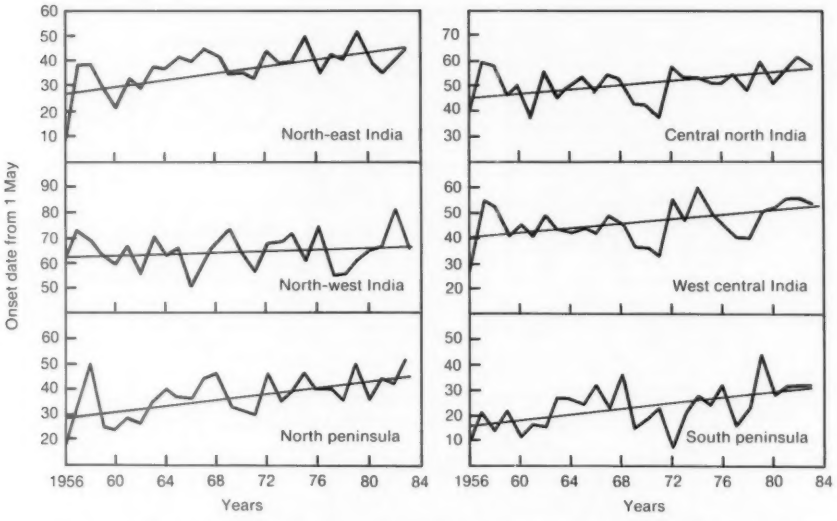

Figure 2. Year to year variations in the dates of onset in different regions of India. The straight line on each graph is the regression line.

such trends could be maintained over long periods. The trends in the first four regions, which are large, are also statistically significant at the 95% level.

In the regions where the trends are small, the rainfall during the onset phase, as well as later, is to some extent accentuated by the westerly troughs, while in the other parts the rainfall entirely depends on the eastern disturbances.

Power spectra of the onset dates for the six regions are presented in Fig. 3. The white-noise null continuum is shown by a horizontal line indicated by NC on each power spectrum. In all the regions there is large power or a peak in the range of 2.0 to 2.5 years. This could be associated with the quasi-biennial oscillation. In north-west India, west central India and central north India prominent power peaks are present in the period 6–8 years. These three regions are contiguous and in the former two the power peaks are significant at the 90% level. In south peninsula there is a peak at 16 years which is also significant at the 90% level. In north-east India and north peninsula there are prominent bands in the range 3–5 years.

3.2 *Snow cover*

The Himalayan, Eurasian and northern hemispheric monthly mean snow covers in the months February to May from 1967 to 1980 and the corresponding linear regressions are presented in Fig. 4. Trends in Eurasian and northern hemispheric snow covers are significant at the 95–99% level, while the Himalayan snow cover trend in May is significant at the 90% level — the trends in other months are not significant. The linear regression indicates an increasing trend of 1–2% of the mean per year in the case of Eurasian and northern hemispheric snow covers, and 0.2–0.9% in the case of Himalayan snow cover. These trends are consistent with the delaying trend in the onset of the summer monsoon over India in view of the accepted fact that heavy snowfall in the western Himalayas in winter has a negative effect on the ensuing monsoon.

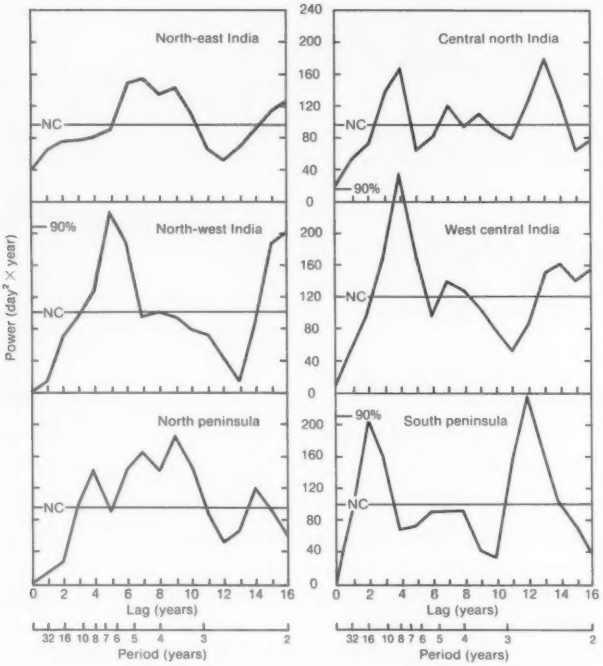

Figure 3. Power spectra of the dates of onset in different regions of India. NC is the null-continuum line. The 90% significant level is indicated where it is relevant.

Power spectra of the snow covers in the 4 months are presented in Fig. 5. All the three regions in February show a significant peak at 5 years. The peak in Himalayan snow cover is significant at the 95% level, while those in the other two are significant at the 90% level. In March and April the spectra are erratic, but in May there is a consistent peak near 2.2 years. It is, however, more pronounced in the northern hemispheric snow cover. A significant peak at 4–5 years is also present in the Himalayan snow in May.

3.3 *Correlations between onset dates and snow covers*

Correlations between onset dates at selected stations and snow covers in different months are presented in Fig. 6. The three snow covers in February show significant positive correlation with onset dates over central India, while in the extreme north-west there is a significant negative correlation. This indicates that the onset tends to be delayed particularly in central India when there is above normal winter snowfall, while it is early over the extreme north-west. In this connection it may be noted that Dey and Bhanu Kumar (1982) found that the period of advance of the monsoon from the southern tip of the Indian subcontinent to the extreme north is smaller in a year in which the Himalayan winter snow cover is large.

In the later spring months the areas of negative and positive correlations shift to the south, and by April and May strong negative correlations are observed in the central parts of the country, especially

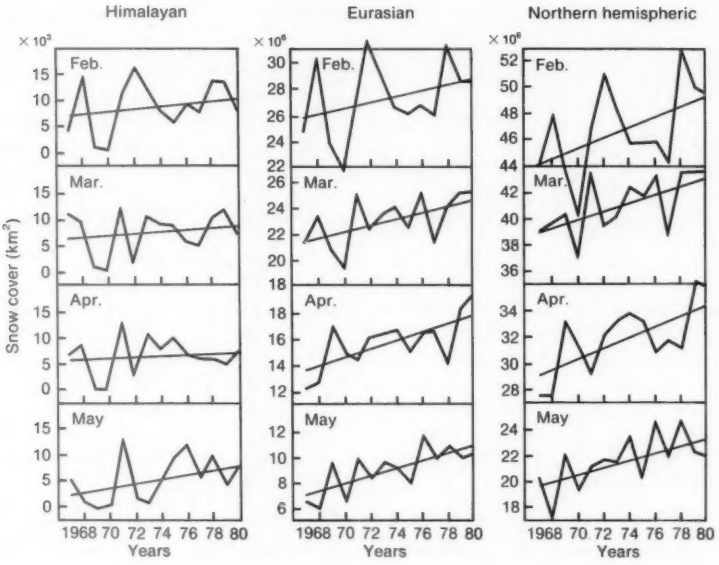

Figure 4. Year to year variations of Himalayan, Eurasian and northern hemispheric snow covers. The straight line on each graph is the regression line.

for the Himalayan snow cover. This indicates that below normal snow cover occurs in April when there is a delayed monsoon. Therefore, there should be rapid snow melt during spring in the years of high snowfall. The correlation between the February snow cover and those in the following months, as well as the snow melts, are given in Table I.

Table 1. *Correlations between February Himalayan snow cover and snow covers in March, April and May. Also the correlations between the February Himalayan snow cover and snow melts from February to March, April and May.*

Snow cover			Snow melt from February to		
March	April	May	March	April	May
0.48	0.28	0.02	0.64	0.70	0.68

The correlations clearly indicate that large snow cover in February is also associated with large snow melt in spring. But the fact remains that large winter snow cover is associated with delayed onset of the monsoon.

It is now known that there has been a warming trend in the northern hemisphere since late nineteenth century till 1940s and cooling thereafter (Budyko 1977, Barnett 1978, Hansen *et al.* 1981, Jones *et al.* 1986a) till early 1970s. Hingane *et al.* (1985) reported a general increasing trend of 0.4 °C per 100 years during 1901–82 in the all-India mean annual temperature. However, their temperature series shows a decrease from early 1950s to early 1970s. These falling trends in temperature in the recent past explain the rising trend in snow covers noted. But the continued rising trend in the snow covers observed in the

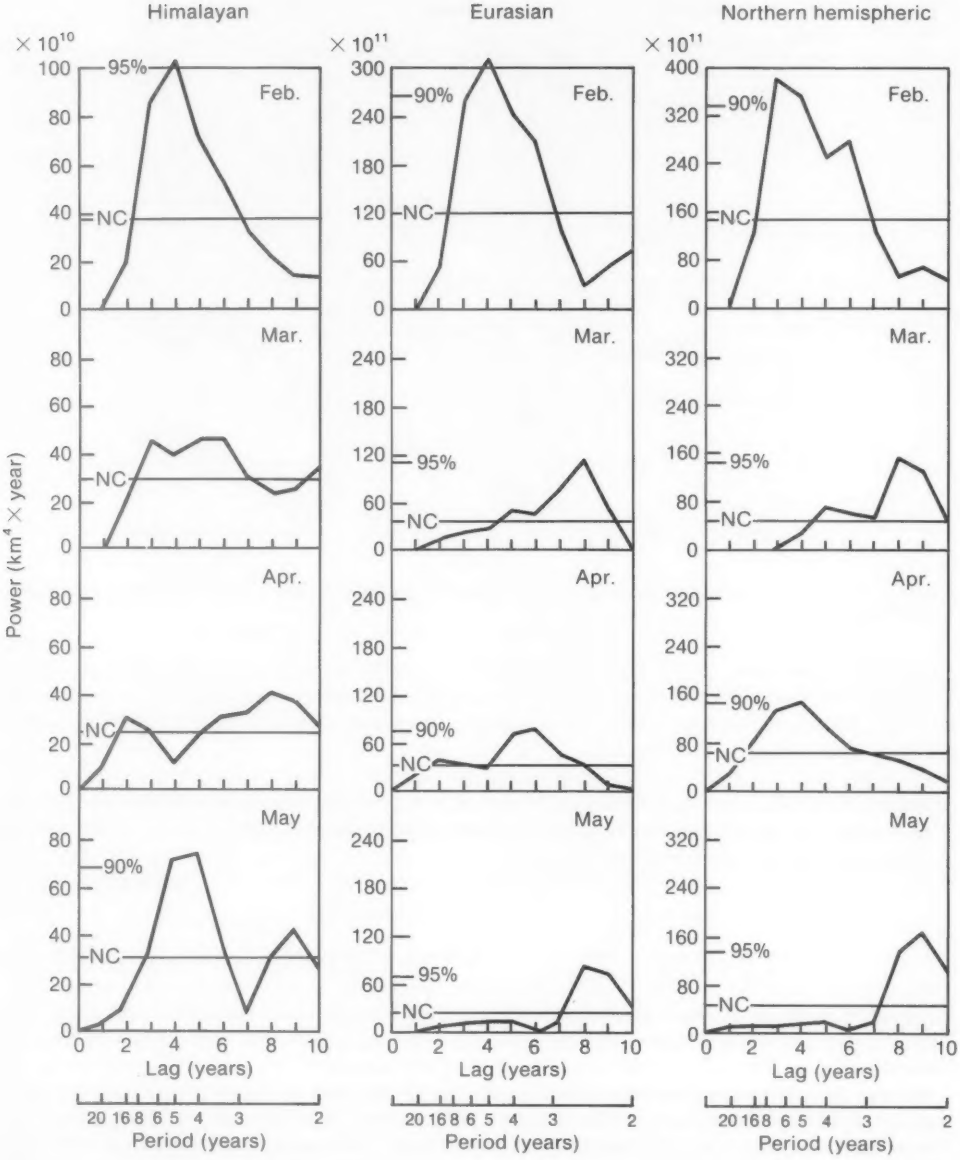

Figure 5. Power spectra of snow covers. NC is the null-continuum line. The 95% and 90% significant levels are indicated where they are relevant.

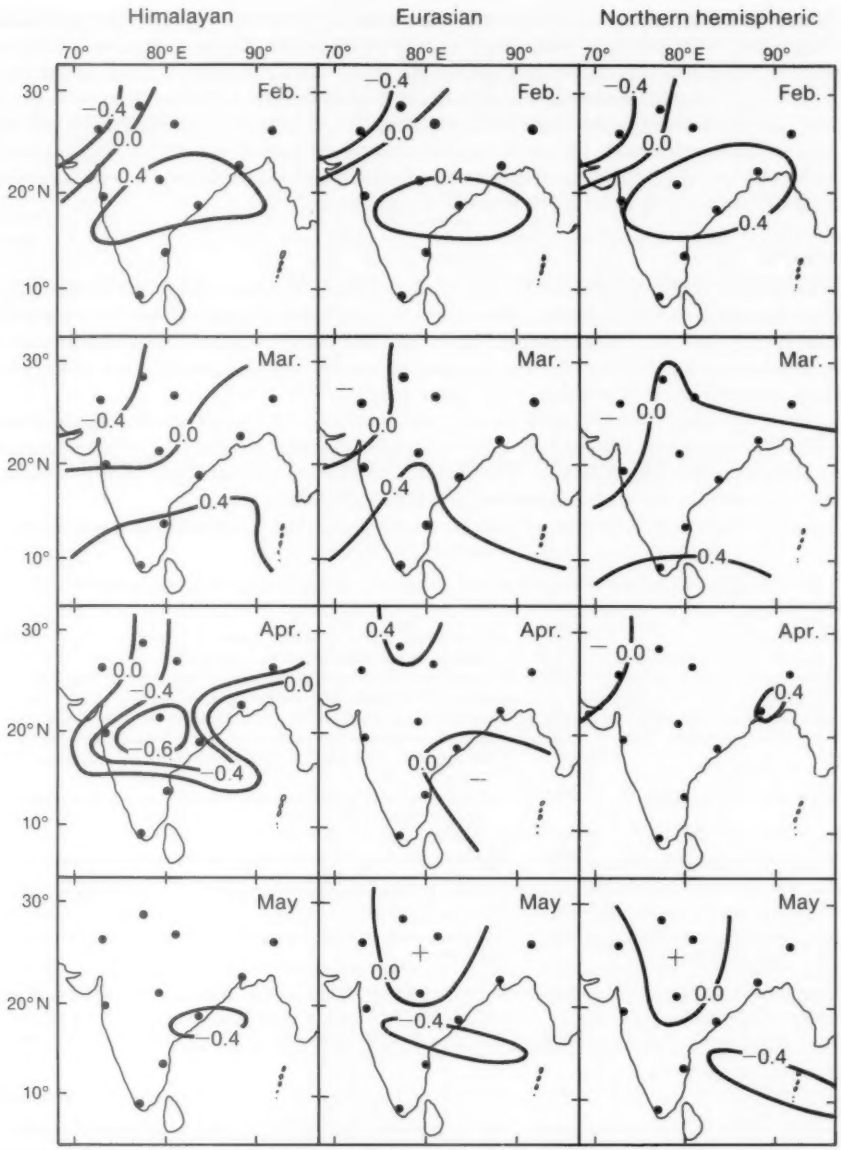

Figure 6. Correlations between Himalayan, Eurasian and northern hemispheric snow covers in different months February to May and the dates of onset at different stations. Locations of the stations are indicated by dots.

present study indicates that it is a more complex phenomenon. Jones *et al.* (1986b) showed that during the cooling phase in the northern hemisphere, i.e. post-1940 period, the temperatures in the southern hemisphere did not have any significant decreasing trend. Also the cooling trend in the northern hemisphere was more in the middle and high latitudes than in the low latitudes. Thus there has been a decreasing trend in the northward temperature gradient. This counteracts the differential heating over south Asia which is responsible for the summer monsoon. Therefore apart from the cooling in the northern hemisphere the differential trends in the northern and southern hemispheres also could be responsible for the delaying trend in the onset of the monsoon.

4. Conclusions

There has been a delaying trend in the onset of the summer monsoon over India during the period 1956–83, and a similar increasing trend in the snow cover over the northern hemisphere, Eurasia and the Himalayas during 1967–80. These trends are consistent with the decreasing trend in temperature of the northern hemisphere as well as India and absence of similar trends in temperature in the southern hemisphere observed by other workers in the recent past.

Power spectra of the onset dates show large power in the 2.0 to 2.5 years which could be associated with the effect of quasi-biennial oscillation. Also, significant power peaks in the 6- to 8-year period in north-west India and the adjoining areas are present, as in a 16-year period in the south peninsula onset dates. For the February snow cover there is a significant period at 5 years.

The snow covers in February show positive correlations with the onset dates, particularly in central India.

References

Ananthakrishnan, R. 1970 The seasonal march of surface pressure gradients across India and the south-west monsoon. *Curr Sci*, **39**, 248–251.

Barnett, T.P. 1978 Estimating variability of surface air temperature in the Northern Hemisphere. *Mon Weather Rev*, **106**, 1353–1367.

Budyko, M.I. 1977 On present-day climatic changes. *Tellus*, **29**, 193–204.

De la Mothe, P.D. and Wright, P.B. 1969 The onset of the Indian south-west monsoon and extratropical 500-mb trough and ridge patterns over Europe and Asia. *Meteorol Mag*, **98**, 145–155.

Dey, B. and Bhanu Kumar, O.S.R.U. 1982 An apparent relationship between Eurasian spring snow cover and the advance period of the Indian Summer Monsoon. *J Appl Meteorol*, **21**, 1929–1932.

Flohn, H. 1964 The tropical easterly jet and other regional anomalies of the tropical circulation. *In* Proceedings of the symposium on tropical meteorology, Rotorua, New Zealand. Wellington, New Zealand Meteorological Service.

Hansen, J., Johnson, D., Lacis, A., Lebedeff, S., Lee, P., Rind, D. and Russel, C. 1981 Climate impact of increasing atmospheric carbon dioxide. *Science*, **213**, 957–966.

Hingane, L.S., Rupa Kumar, K. and Ramana Murty, Bh. V. 1985 Long-term trends of surface air temperature in India. *J Climatol*, **5**, 521–528.

Jones, P.D., Raper, S.C.B., Bradley, R.S., Diaz, H.F. Kelly, P.M. and Wigley, T.M.L. 1986a Northern hemisphere surface air temperature variations: 1851–1984. *J Clim and Appl Meteorol*, **25**, 161–179.

Jones, P.D., Raper, S.C.B. and Wigley, T.M.L. 1986b Southern hemisphere surface air temperature variations: 1851–1984. *J Clim and Appl Meteorol*, **25**, 1213–1230.

Koteswaram, P. 1958 The easterly jet stream in the tropics. *Tellus*, **10**, 43–57.

Kung, E.C. and Sharif, T.A. 1981 Long-range multi-regression forecasting of the Indian summer monsoon onset and rainfall with antecedent upper air pattern and sea surface temperature. *In* International conference on early results of FGGE and large-scale aspects of its monsoon experiments, Tallahassee, Florida. Geneva, WMO.

Maruyama, T.	1968	Time sequence of power spectra of disturbances in the equatorial lower stratosphere in relation to the quasi-biennial oscillation. *J Meteorol Soc Jpn*, **46**, 327–342.
Maung Tun Yin	1949	A synoptic–aerologic study of the onset of the summer monsoon over India and Burma, *J Meteorol Am Meteorol Soc*, **6**, 393–400.
Mitchell, J.M., jun., Dzerdzeevskii, B., Flohn, H., Hofmeyr, W.L., Lamb, H.H., Rao, K.N. and Wallén, E.C.	1966	Climatic change, Technical Note No. 79. Geneva, WMO.
Ramamurthi, K.M. and Keshavamurty, R.N.	1964	Synoptic oscillations of Arabian anticyclones in the transition season. *Ind J Met Geophys*, **15**, 227–234.
Subbaramayya, I. and Bhanu Kumar, O.S.R.U.	1978	The onset and the northern limit of the south-west monsoon over India. *Meteorol Mag*, **107**, 37–48.
Subbaramayya, I., Babu, S V. and Rao, S.S.	1984	Onset of the summer monsoon over India and its variability. *Meteorol Mag*, **113**, 127–135.

551.5:06(b)

Atmospheric research at the University of Manchester Institute of Science and Technology

C.P.R. Saunders

Department of Pure and Applied Physics, University of Manchester Institute of Science and Technology

Summary

This article gives brief descriptions of the research activities being carried out in the Department of Pure and Applied Physics at the University of Manchester Institute of Science and Technology. These include acid-rain studies at our field research station, the development of instrumentation for use in the field and on our instrumented aircraft which has flown in studies of maritime aerosol over South Uist, computer modelling of cloud development, a novel radar technique to discriminate between water and ice in clouds and a long-term investigation of thunderstorm electrification processes.

1. Introduction

The University of Manchester Institute of Science and Technology (UMIST) atmospheric physics group is in its 25th year. Founded by J. Latham, who brought with him from Imperial College, London an interest in thunderstorm electrification, the group now comprises over 40 people and, while the initial interests remain, research is now quite diverse. The group has research facilities in UMIST and at Great Dun Fell (GDF) in Cumbria, and it possesses an instrumented van and aircraft. Although laboratory-based work continues, recent emphasis has been in the field where our own instrument design and development has played an important role. Several members of the group have contributed résumés of their present studies which have been incorporated in this article to give the reader a broad outline of the work in hand. Some of our recent papers are listed in the references and bibliography section at the end.

2. Acid rain

A major experiment to investigate cloud chemical processes and the variation with altitude of wet deposition is being conducted at GDF in collaboration with the Department of Chemistry at UMIST, the Department of Environmental Sciences at the University of East Anglia, the Environmental Sciences Division at the Atomic Energy Research Establishment at Harwell and the Institute of Terrestrial Ecology (ITE) at Penicuik. Great Dun Fell is 847 m above sea level and forms part of the long

ridge of the Pennine Hills, which runs from north-west to south-east, and lies to the north-east of the Eden valley. The prevailing south-west winds blow almost at a right angle to the ridge and form a cap cloud which envelops the site for parts of 250 days per year. The experiments performed to date have concentrated on the aqueous-phase oxidation of sulphur dioxide by hydrogen peroxide and ozone and also the deposition by rain-out (by the seeder feeder mechanism) of chemical species incorporated in the cloud droplets by nucleation scavenging or aqueous-phase chemistry. In collaboration with the Central Electricity Research Laboratories a series of experiments is also being conducted in which a plume of sulphur dioxide gas with sulphur hexafluoride tracer is released in the valley bottom and targeted on the summit. Collaboration is also being sought with the Department of Botany at the University of Manchester to investigate the effects of the deposition on the vegetation at GDF.

The experiments are centred on three sites; Fig. 1 shows the deployment of the apparatus. At site 1, the airstream upwind of the cloud is monitored for hydrogen peroxide, sulphur dioxide and ozone in the gas phase; the atmospheric aerosol is captured using an impactor and the size distributions of the hygroscopic particles are measured. Rainfall is measured and collected for chemical analysis. Site 2, the van site, is the mobile laboratory where gas-phase sulphur dioxide and ozone are measured, together with the cloud liquid-water content and droplet size distribution. Cloud water is collected for the continuous monitoring of acidity (pH) and aqueous-phase hydrogen peroxide using a luminol technique; separate samples are stored for later analysis by ion chromatography. An accoustic sounder is located at site 3 (for the remote sensing of the cloud top where entrainment is expected), together with a sonic anemometer for turbulence and occult deposition measurements. All site 2 measurements are repeated at site 3. In addition, cloud-water collectors are positioned at eight other sites on the hillside along with ITE rain-water collectors for hydrogen peroxide measurements and ion chromatography for the major anions and cations. The measurements have shown that when significant concentrations of sulphur dioxide are present in the airstream the hydrogen peroxide dissolved in the cloud water is consumed at a rate consistent with that predicted by recent laboratory studies.

When the cloud is affected by dry air entrainment from aloft, extra hydrogen peroxide is introduced. The results suggest that the concentration of hydrogen peroxide in the free tropospheric air entrained may be several times greater than that in the boundary-layer air in which the cloud forms. The reaction rate data suggest that the hydrogen peroxide–sulphur dioxide reaction is fast and is likely to be oxidant-limited. Consequently in many conditions, when oxidation by hydrogen peroxide is dominant

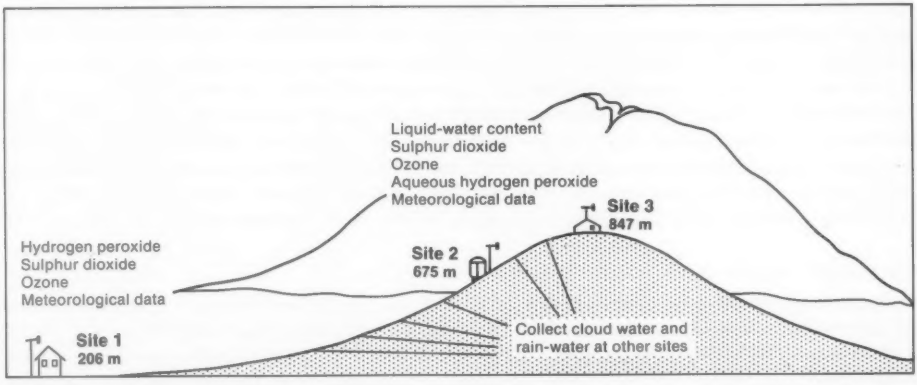

Figure 1. Locations of the three experimental sites on Great Dun Fell showing the elements measured at each.

over ozone due to low cloud-water pH, the rate of sulphate production may be controlled by the rate at which hydrogen peroxide can be entrained into a cloud system.

In the experiments carried out in November 1986 no significant sulphate production was observed. This is consistent with the very low hydrogen peroxide concentrations observed (equivalent to typically around 5 parts per thousand (by volume) in the gas phase), however, during the spring months hydrogen peroxide concentrations typically one hundred times greater than this have been detected using the same instrumentation. In these conditions significant sulphate production is observed.

A marked increase in the concentrations of the major ions in rain is found with altitude. On average, concentrations increase by a factor of two between 250 and 847 m. The increase in rainfall by a similar factor leads to a wet deposition rate of most ions at the summit of four times that at the valley sites. These changes can be accounted for by a quantitative description of the seeder feeder process in which the hygroscopic aerosol particles are incorporated into the feeder cloud droplets by nucleation scavenging and are then efficiently washed out by the raindrops entering the cloud from the seeder cloud above.

3. Instrumentation

The total water mixing ratio is an important parameter in understanding the interaction of a cloud with its environment since it provides information about the origin of air entrained into the cloud. This has provided the stimulus for the development of instruments to measure total water content, and a significant fraction of the group's instrumentation work has recently been directed to this end. Two approaches have been tried. The first uses rapid-response carbon hygristors to monitor cloud air sampled via an evaporator. This provides considerable temporal resolution but, in its most basic form, is subject to the poor long-term stability of this type of sensor. As a consequence the latest versions of this instrument incorporate an automatic re-calibration facility which largely eliminates this problem. The second approach involves a direct capacitive measurement of water vapour content which is potentially capable of faster response than the former technique. The hygristor-based instrument, in addition to its intended use in ground-based cloud evolution studies, has recently been used in the UMIST marine aerosol work to provide dew-point data. Since the sensor is operated at elevated temperatures it is less prone to salt contamination than the cooled-mirror type dew-point instrument used previously. The instrument is also being used on the Natural Environment Research Council HEXOS (Humidity Exchange Over the Sea) marine boundary-layer project to provide information on the vertical transport of water vapour.

4. Research aircraft

The research group operates a Cessna 182 aircraft for studies in cloud physics, atmospheric chemistry, aerosol physics and boundary-layer dynamics. The aircraft is flown with a crew of two and carries an equipment payload of up to 200 kg. Its flight performance permits measurements to be made up to an altitude of 6 km at air speeds in the range 25–27 m s^{-1} and the aircraft can remain airborne for up to 6 hours. To enable a wide range of measurements to be made in flight, certain modifications have been made to the aircraft. All internal equipment is installed on a single removable tray which fills the rear seat and luggage area and facilitates equipment changes. Two attachment points, one under each wing outboard of the propeller, are used to mount particle-sampling probes and other external sensors. Air-sampling intakes on the wing provide an isokinetic supply for a particle-sampling probe, a fast-response humidity sensor and a dew-point hygrometer via an air deceleration system. The electrical power available has been increased by converting the aircraft to 28 V, installing a 95 A alternator and a static inverter to provide 115 V a.c. Other parameters measured include air temperature from both Rosemount and reverse-flow thermometers, pressure altitude, radar altitude and air speed. The aircraft's position is obtained by recording signals from on-board equipment. The computer-based data

acquisition system permits in-flight display of any parameter and data are recorded on to industry-standard magnetic tape.

5. Maritime aerosol

Field studies of maritime aerosol particles have been pursued by UMIST since 1979 in an attempt to characterize aerosol over the North Atlantic under a variety of meteorological conditions. Measurements, primarily with particle-sizing instruments covering the radius range 0.1 to 150 μm, have been made for several periods on the coast of South Uist in the Outer Hebrides, which possesses a relatively undisturbed exposure to the prevailing westerly winds. Initial measurements were undertaken in collaboration with a team from the Royal Aircraft Establishment, Farnborough, and other field projects have involved a Dutch team and flights by the Hercules aircraft of the Meteorological Research Flight. These studies have clearly demonstrated the dominant influence of wind speed on particle production at the sea surface and have also illustrated the effects of relative humidity and the depth of the atmospheric mixed layer upon the observed particle concentrations and size distribution (Exton *et al.* 1985). More recently, work has commenced at UMIST on the development of a simple maritime atmospheric boundary-layer model capable of predicting the particle concentrations throughout the mixed layer on the basis of the prevailing meteorological conditions. As a part of this programme, measurements made at South Uist over the past year have involved the UMIST instrumented aircraft as well as ground-based measurements. During August 1986, the aircraft flew for a total of about 50 hours over the sea, gathering data on particle concentrations and meteorological variables to provide vertical and horizontal profiles from 20 m up to cloud base. Also, UMIST had the good fortune (despite the damage sustained to various vehicles and equipment) to be present on the islands during the gales of March 1986 when particulate measurements were obtained with wind speeds approaching 100 m.p.h. Data from these projects are still being analysed.

6. Atmospheric modelling

For the last 10–15 years, fluid problems in plasma and astrophysics have been modelled by simulating a fluid as a collection of incompressible particles of defined radii (Monaghan 1985). However, this Lagrangian element approach (or 'smooth-particle hydrodynamics') has not been applied to fluid-flow atmospheric modelling. Conventional finite difference, spectral or finite element analyses use a Eulerian frame fixed relative to the earth's surface. UMIST research intends to simulate numerically some atmospheric fluid-flow problems by means of this novel technique. It is hoped that, for the case of atmospheric fluid flow, full advantage can be made of the ability to trace the fluid elements around a dynamical system. Water vapour and liquid water are carried around by the fluid elements. The 'blob-like' nature of clouds provides one of the main reasons for using this particular approach. It is also clear that more detailed microphysics could be included into these elements at a later date. However, there are problems with the representation of the thermodynamics in general, and the temperature gradients in particular. In addition the energy is transferred around the system by a series of 'shocks', which produce certain restrictions on the time step and tolerance required. The implicit advantages of using the system of ordinary differential equations, especially when compared with the numerical manipulations involved in obtaining the solutions for partial differential equations, lie in the well-studied stability criteria and error prediction which are available in the current numerical analysis literature. These studies have some similarities to other Lagrangian approaches (Cullen and Purser 1984) which are currently being investigated at other institutions.

At present it is felt that the model is in a suitable state to simulate two-dimensional cumulus cloud development in a 4 km wide box. A stable atmospheric ground state has been achieved, and the current simulation involves gradually increasing the boundary-layer (< 500 m) temperature. It is anticipated,

from the previous low-resolution test computations, that convection on different length scales will start to develop. It should be possible to examine, for example, the processes of fluid entrainment. There is a possibility that, if successful, there could be some collaboration with other scientists who are considering an observational programme of the same phenomena. A further long-term plan is to use the model and other numerical techniques to study flow over quasi two-dimensional ridges, using for comparison the measurements from the UMIST field station at GDF.

7. Radar

A new radar technique, using differential reflectivities, makes it possible to distinguish between raindrops and ice particles, to measure the mean size of raindrops and to make more accurate estimates of rainfall by remote sensing. The method was developed by our collaborators at the Rutherford Appleton Laboratory. Observations are made on the 25 m diameter antenna at Chilbolton, Hampshire, which has a beam width of only a quarter of a degree and is the largest steerable meteorological radar in the world. A conventional radar measures the back-scattered power, which is proportional to ND^6 (where N is the concentration of particles of size D) summed over all particle sizes. This power is generally expressed as the radar reflectivity factor, Z, which is the power in decibels (dB) relative to the power which would be scattered by one spherical raindrop of diameter 1 mm per cubic metre (the units of Z are denoted by dBZ). Fig. 2(a) shows values of Z in a vertical section through an active cumulonimbus. The heaviest precipitation is evidently at a range of about 87 km where Z exceeds 60 dBZ (i.e. Z is above 10^6 mm^6 m^{-3}). Various empirical relationships are available to convert Z into a rainfall rate, R, but these are not very accurate because the same rainfall rate can arise from various raindrop-size distributions which would have very different values of ND^6. An additional ambiguity arises because liquid water is a much better microwave scatterer than ice, but from Z alone we have no way of knowing whether the particles are raindrops or frozen hydrometeors.

The differential radar reflectivity measurements, Z_{DR}, can resolve some of these ambiguities. It is defined as $10 \log(Z_H/Z_V)$ where Z_H and Z_V are the radar reflectivity factors measured for horizontally and vertically polarized radiation. The shape of a raindrop is a unique function of its size; if the diameter is less than 1 mm, raindrops are essentially spherical so that Z_{DR} will be zero; larger raindrops are increasingly distorted so that Z_{DR} is positive with a magnitude which is a measure of the mean raindrop size. For ice particles the situation is more complicated, but in convective clouds the graupel particles and hailstones tend to tumble as they fall, so that on average Z_{DR} is zero. These interpretations of the radar signals have been confirmed by direct sampling of the precipitation particles using the Meteorological Research Flight C-130 Hercules aircraft (Bader *et al.* 1987, Cherry *et al.* 1984).

The values of Z_{DR} in Fig. 2(b) were taken simultaneously with Z. The freezing level on this day was at about 3 km; above this height Z_{DR} is essentially zero for all values of Z, suggesting that the particles are all frozen. Positive values are confined to regions below 3 km where the ice has melted to form aspherical raindrops, with a tendency for larger drops where Z is greater. If Z and Z_{DR} measurements are both available, then it is possible to estimate a mean raindrop size from Z_{DR} and, once the size is known, the concentration may be computed from Z. Knowing both the size and concentration of the raindrops leads to greater accuracy in rainfall estimates than those possible from Z alone. Of particular interest in the figure is a narrow region at a range of 87 km where zero values of Z_{DR} extend right down to the ground; it is believed that this is where hailstones are falling to the ground. Any interpretation in terms of small spherical raindrops would require unrealistically large concentrations to give the observed Z, with an equivalent rainfall rate of many millimetres per hour. This method appears to provide the first reliable way of identifying hail by radar, and further observations should show if it is possible to track the movement and development of hail swaths. Observations during the vigorous growth of convective clouds reveal transitory regions containing large supercooled raindrops where the temperature is as low

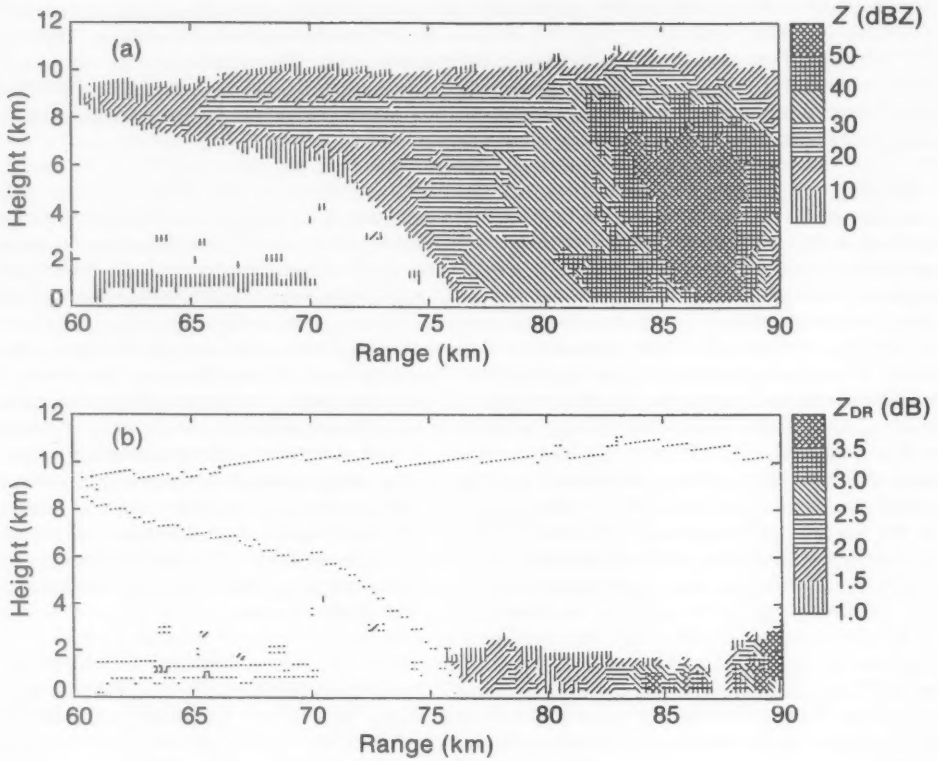

Figure 2. Contour plots of radar reflectivity (Z) and differential reflectivity (Z_{DR}), obtained from a vertical scan through an intense convective storm at 1336 GMT on 6 July 1983. (a) Z values expressed in dBZ above 1 $mm^6 m^{-3}$. (b) Z_{DR} values in dB. To delineate the extent of the echo, the dotted lines taken from (a) surround the area where Z exceeds 0 dBZ. Hatching is used to denote areas where Z_{DR} exceeds +1 dB. The positive values of Z_{DR} below 2 km altitude are due to large raindrops falling with their horizontal axis larger than the vertical.

as −10 °C. Such regions would be hazardous to sample using an instrumented aircraft. The differential-reflectivity technique works well for water drops because the raindrop shape is a unique function of its size, but problems remain with ice particles which can be of different sizes, shapes, densities and fall modes. Further observations in 1987 with additional polarization parameters should remove some of these ambiguities.

8. Thunderstorm electrification

Laboratory studies of thunderstorm electrification processes have long been a major interest in the group. Over the last few years these have continued with the addition of collaborative field studies in the USA. Using cold rooms, thunderstorm conditions are simulated and ice crystals are made to collide with ice targets which represent soft-hailstones. During the collision and separation events, electrical charge is transferred. Comprehensive experiments covering a wide range of conditions have now shown that the

sign and magnitude of the charge transfer is a function of the temperature, the ice crystal size, the impact velocity, the liquid-water content in the cloud and the impurity concentration in the droplets. This wide range of controlling parameters has meant that previous studies which have perhaps ignored some of the variables have produced conflicting results. The present work has now made the measurements reproducible by careful control of all the cloud conditions. In general, the results can be summarized as follows:

(a) adequate charge transfer to explain thunderstorm electrification requires ice crystal/soft-hailstone interactions to take place in the presence of supercooled water (crystals alone separate negligible charge),

(b) at temperatures above about −20 °C the soft-hailstone charges positively, while at lower temperatures it charges negatively, and

(c) the temperature at which the charge sign reversal takes place is controlled by the liquid-water content, so that higher liquid-water contents favour positive charging of the soft hail.

Thus, in a thunderstorm, charge transfer at high levels leads to negatively charged soft hail pellets which fall to form the negative charge region while the positive crystals are carried aloft. At lower levels, with reversed charging, the negative crystals are levitated and contribute to the negative region while the positive soft hail falls to form a lower positive-charge region. Such cloud electrification has been observed and there is increasing evidence that this conceptual model of charges on cloud particles is correct. Remote sensing has shown that lightning is often initiated from the level of charge sign reversal where the negative charges reside in regions of high radar reflectivity (Krehbiel *et al.* 1979). Collaborative flights in the USA have confirmed that charges exist on cloud particles in the boundaries between updraughts and downdraughts where maximum particle collision rates would be expected (Dye *et al.* 1986). However, the mechanism of charge transfer remains to be elucidated; work suggests that the sign is closely controlled by the precise conditions at the surfaces of both the interacting particles. Our aim is to completely resolve this question.

9. Concluding remarks

Over the years the interests of the research group have diversified considerably and no doubt this trend will continue as new questions arise and new interests are aroused. Nevertheless, throughout the group there is a strong unanimity of purpose, which is to help solve some of the outstanding problems in atmospheric physics.

Acknowledgements

The contributors to this article are T.W. Choularton, A. Gadian, M.J. Gay, A.J. Illingworth, C.S. Mill, M.H. Smith and I.M. Stromberg.

References and bibliography

Bader, M.J., Clough, S.A. and Cox, G.P. 1987 Aircraft and dual polarization radar observations of hydrometeors in light stratiform precipitation. *Q J R Meteorol Soc*, **113**, 491–515.

Baker, B., Jayaratne, E.R., Latham, J. and Saunders, C.P.R. (1987) The influence of diffusional growth rates on the charge transfer accompanying rebounding collisions between ice crystals and soft-hailstones. (Submitted to *Q J R Meteorol Soc.*)

Carruthers, D.J. and Choularton, T.W. 1982 Airflow over hills of moderate slope. *Q J R Meteorol Soc*, **108**, 603–624.

1986 The microstructure of hill cap clouds. *Q J R Meteorol Soc*, **112**, 113–129.

Chandler, A.S., Choularton, T.W., Dollard, G.J., Gay, M.J., Hill, T.A., Jones, A., Jones, B.M.R., Morse, A.P., Penkett, S.A. and Tyler, B.J. (1987) A field study of cloud chemistry and cloud microphysics at Great Dun Fell. (Submitted to *Atmos Environ.*)

Cherry, S.M., Goddard, J.W.F. and Ouldridge, M.	1984	Simultaneous measurements of rain by airborne distrometer and dual-polarization radar. *Radio Sci*, **19**, 169–176.
Choularton, T.W., Consterdine, I.E., Gardiner, B.A., Gay, M.J., Hill, M.K., Latham, J. and Stromberg, I.M.	1986	Field studies of the optical and microphysical characteristics of cloud enveloping Great Dun Fell. *Q J R Meteorol Soc*, **112**, 131–148.
Cullen, M.J.P. and Purser, R.J.	1984	An extended Lagrangian theory of semi-geostrophic frontogenesis. *J Atmos Sci*, **41**, 1477–1497.
Dye, J.E., Jones, J.J., Winn, W.P., Cerni, T.A., Gardiner, B., Lamb, D., Pitter, R.L., Hallett, J. and Saunders, C.P.R.	1986	Early electrification and precipitation development in a small, isolated Montana cumulonimbus. *J Geophys Res*, **91**, 1231–1247.
Exton, H.J., Latham, J., Park, P.M., Perry, S.J., Smith, M.H. and Allan, R.R.	1985	The production and dispersal of marine aerosol. *Q J R Meteorol Soc*, **111**, 817–837.
Hill, T.A. and Choularton, T.W.	1985	An airborne study of the microphysical structure of cumulus cloud. *Q J R Meteorol Soc*, **111**, 517–544.
Hill, T.A., Choularton, T.W. and Penkett, S.A.	1986	A model of sulphate production in hill cap cloud and subsequent turbulent deposition onto the hill surface. *Atmos Environ*, **20**, 1763–1773.
Illingworth, A.J., Goddard, J.W.F. and Cherry, S.M.	1987	Polarization radar studies of precipitation development in convective storms. *Q J R Meteorol Soc*, **113**, 469–489.
Jayaratne, E.R., Saunders, C.P.R. and Hallett, J.	1983	Laboratory studies of the charging of soft-hail during ice crystal interactions. *Q J R Meteorol Soc*, **109**, 609–630.
Krehbiel, P.R., Brook, M. and McCrory, R.A.	1979	An analysis of the charge structure of lightning discharges to the ground. *J Geophys Res*, **84**, 2432–2456.
Monaghan, J.J.	1985	Particle method for hydrodynamics. *In* Computer physics reports. Amsterdam, North-Holland Publishing.

An appreciation of the work of Mr D.E. Miller

K.H. Stewart

Director of Research, 1976–82, Meteorological Office, Bracknell

I worked very closely with Derek Miller for over 15 years, so I would like to complement the retirement notice in the last issue of this magazine with my own appreciation of Derek's work.

I first met Derek Miller when in 1959 he came to Kew from forecasting at London (Heathrow) Airport. He was certainly one of the first, perhaps the very first, full-time member of Met O 19 (now the Satellite Meteorology Branch). The task was to devise and construct equipment to measure ozone from the Ariel 2 satellite, within about 3 years, and a rocket version of the equipment had to be made and flown even earlier. The range of topics to be covered, problems to be solved and techniques to be mastered seemed, at times, to cover almost the whole range of classical physics, and the group was so small that everyone had to be aware of and contribute to all aspects. Derek's contributions and the stimulus provided by his keen and enquiring mind were outstanding, but even more important was the speed and thoroughness he showed in translating sketchy ideas into working hardware, with all peculiarities and imperfections explored and understood. His masterpiece was the no-moving-parts spectrometer to scan the spectrum from 250 to 400 n mile by the rotation of the rocket or satellite. In order to complete the detailed optical design of this, he was detached for a few weeks to the optical department of the Imperial College of Science and Technology, London; my impression is that he returned with a better understanding of practical ray-tracing than the staff at the College!

Another essential development was that of the test equipment for photometric measurements in the ultraviolet. This began as a fairly simple piece of commercial equipment but was developed over the next decade or so into an elaborate system of great versatility and, in Derek's hands, high precision, for measurements on a wide range of sensors.

In 1963 the satellite equipment was taken to the USA for 'integration' and testing. Derek spent several lengthy periods there and won considerable respect — not always liking — from the Americans for his thoroughness, his tenacious regard for the requirements of our experiments and the breadth and depth of his knowledge.

Unfortunately, early rocket and satellite experiments fell far short of total success. The main reasons were that the spinning motions of the vehicles were by no means as simple and regular as we had expected and that optical surfaces became contaminated, probably by out-gassing from surrounding materials.

The rest of the 1960s was spent in further rocket experiments (water vapour as well as ozone) in which these difficulties were gradually overcome, and in painstaking analysis of the flawed results of the earlier experiments. Derek's few papers on this work contain some valuable data but are chiefly impressive (in contrast with much other published work) for the completeness with which they analyse and overcome the difficulties and errors of the 'occultation' technique. Derek succeeded in rescuing a considerable amount of ozone data from the satellite experiment but could never be persuaded to publish this, because it had to be based on assumptions which were reasonable but whose validity could not be proved beyond question.

The next development was Derek's work in connection with Meteosat, beginning in the early 1970s. He did valuable work on many committees and working groups but his biggest contribution was to the study that defined the requirement for, and to a large extent the methods to be used by, the Ground Facility for a Geostationary Meteorological Satellite. This study laid the foundations for the effective exploitation of Meteosat data. It was the work of a very small group, including some of the brightest rising stars of the European Meteorological Services. I have the impression that Derek formed closer friendships within this group than within the Office, perhaps because the contacts were occasional and the project free of petty restrictions. Certainly he was, and is, regarded in European Space Agency (ESA) circles with great respect and, I think, affection.

Looking back on Derek's career, it seems to me the constant thread (against a background of first-class physical insight) has been a great thoroughness and a desire to master the details of every task, not in any dull and stodgy sense but with a keen spirit of enquiry that drives him to explore and understand every aspect. In the early days his fault was an unwillingness to delegate work or accept help — he found it quicker to do a job himself than to explain what needed doing. He was also so deeply immersed in his immediate project that he had little time or opportunity to relate it to the wider work of the Office. Over the years he has come to accept that people less bright and dedicated than himself have an essential contribution to make and has taken a steadily increasing interest in the work of the Office as a whole. All this, you might say, is no more than the normal development of a career and a personality, but my impression is that Derek started further back and has travelled further forward than most. He responded with enthusiasm to the increasing opportunities to apply to the mainstream work of the Office the expertise and authority in space matters he had acquired in his earlier work on the fringes of meteorology. In his work with ESA, and later as Assistant Director (Satellite Meteorology), to ensure that data from space were exploited to the full and made available to forecasters in the form best suited to their needs, his advocacy of the wider and fuller use of satellite data was all the stronger for his depth of understanding of the practicalities of the forecasting task.

Although I did not see it at first hand, I know that his horizons continued to expand over the last few years and that the qualities I admired in the early days have been evident in all his tasks.

Reviews

The elements of graphing data, by W.S. Cleveland. 164 mm × 233 mm, pp xii + 323, *illus*. Monterey, California, Wadsworth Advanced Books and Software, 1985. Price £20.85 (paperback).

This book aims to show us how to present data graphically in the clearest possible manner. The author points out that graphs are used in science and technology, both to help analysis and understanding of data, and to communicate the data to others.

Examples are given of badly-designed graphs (including some real howlers) from published papers. Many are reworked to show how they might have been better presented. The range of fields subjected to the author's scrutiny is huge: papers with titles ranging from 'Modulation of atmospheric carbon dioxide by the Southern Oscillation' to 'Transglutaminase-mediated modifications of the rat sperm surface in vitro' figure in the book.

The author goes on to discuss the basic elements of graph construction: tick marks, scales, legends, symbols, labels, etc. He makes the point that even such elementary features are often given insufficient thought, and suggests rules-of-thumb in their use.

The next chapter deals with graphical methods and introduces some ways of displaying data which are astonishingly new — the 'scatterplot matrix' for example was first discussed in the literature in 1983. Other techniques deserving consideration are:

(a) the Tukey sum-difference graph,
(b) Lowess — robust locally weighted regression (a smoothing technique),
(c) the Tukey box graph — indicates variation of measurements more effectively than error bars.

Finally the author deals with graphical perception — how accurately can the brain analyse different methods of representing data magnitudes (distance, area, angle, slope, shading density, colour hue, etc.).

Cleveland deals admirably with these topics, but one unfortunate omission (for us) is that contour maps are not discussed. Moreover, a few minor points he makes are open to question in my mind. Nevertheless, there is much here to provoke thought and encourage high standards of presentation of data.

Ideally, everyone interested in getting the most out of their data or presenting data clearly and concisely should have a copy handy.

T.S. Hills

Remote sensing digital image analysis, by J.A. Richards. 168 mm × 248 mm, pp. xvii + 281, *illus*. Berlin, Heidelberg, New York, London, Paris and Tokyo, Springer-Verlag, 1986. Price DM 138.00.

This book sets out to fill a gap between those texts on remote sensing and its applications, which treat digital analysis methods superficially, and those which are too mathematically detailed for the non-specialist to find of practical use. This gap certainly existed in the past, but this book succeeds in bridging it. It covers most of the topics encountered in remote sensing image analysis in a way which leaves the reader confident of being able to tackle such problems. Part of its success is in assuming little prior knowledge: there are appendices covering satellite orbits, vector and matrix algebra, fundamentals of probability and statistics, and even binary representation of numbers. However, the main reason this book is such a good introduction to the subject is not these useful appendices, but the many examples given throughout the text. In each chapter, a discussion of general principles is followed by numerical examples in sufficient detail that a reader could repeat the calculations and check them at every stage.

Where there are alternative solutions to a problem they are compared in terms of algorithm complexity and quality of results. Between five and ten problems are posed at the end of each chapter and have been selected to permit solutions to be obtained without recourse to a computer. Reference lists are provided for each topic and include a useful preamble comparing and contrasting the value of different references for different applications.

The topics covered include descriptions of specific satellite-borne instruments, error correction and image registration, contrast enhancement and geometric enhancement, multi-spectral transformations, Fourier transformation and several chapters on aspects of classification including supervised and unsupervised techniques, feature reduction, and practical strategies for classifying images. The depth to which each topic is explored is probably sufficient for anyone for whom image analysis is only part of their work. There are sufficient references for those who require more detail and there is advice on which references are most useful. Although the book maintains a good degree of generality there is a tendency to concentrate on the use of LANDSAT data in agricultural/ecological applications. From the point of view of a meteorologist there are a few disappointments about the book. The gross empiricism used in the correction of atmospheric effects and the definition of transmittance that leads to its dependence on zenith angle may offend the purist. The absence of any treatment of pattern matching, as used in cloud tracking, might be expected in an introductory text but the almost synonymous use of 'spectral' space and 'feature' space obscures the use of image properties such as texture as features in classification procedures.

There are a few minor irritations in the presentation of the book. In some chapters the number of typesetting errors is rather high. While this is little more than an annoyance in the text it can be quite serious in equations as in 5.2 where the convolution operation is wrongly defined. The index contains many entries which redirect the reader (e.g. Fourier Transformations, fast — see Fast Fourier transform). It is difficult to understand why publishers do this when it would be simpler to include the page number. For a relatively expensive book (DM 138 = £47.50) printed on very high quality paper the cover is extremely disappointing. In a subject as full of exciting imagery as remote sensing one might expect more than a monochrome representation of an image produced on a line printer! There are, nevertheless, some very good colour images inside.

It is customary to assume that books at this price will be purchased mostly by libraries but in this case that would be a pity. In spite of the cost I would recommend it to researchers and post-graduate students who use image analysis techniques and I am confident that it will quickly take on a well-thumbed appearance.

C. Duncan

Books received

The listing of books under this heading does not preclude a review in the Meteorological Magazine at a later date.

Statistical analysis of spherical data, by N.I. Fisher, T. Lewis and B.J.J. Embleton (Cambridge University Press, 1987. £35.00, US $65.00) aims to present a unified and up-to-date account of the methods of analysis of data in the form of directions in space. The emphasis is on applications of the statistical methods to the many relevant fields.

Satellite photograph — 6 August 1987 at 1359 GMT

The visible image shows the distribution of convective cloud over central and southern Britain on a day when marked sea-breezes were present within a cyclonically-curved, weak, west to north-west airflow.

Over southern England only small cumulus are present, except adjacent to the south coast where, according to surface observations, a sharp sea-breeze front had developed. The convergence line may be inferred from the image as being along the northern limit of the cloud area covering extreme southern England, and lies close to the coast in the west, but well inland over south-east England. Individual convective cells moved downwind (east to east-south-eastwards) towards the English Channel where they dispersed.

In contrast to the cloudiness over south-east England, the coastal strip of north-east France and the Low Countries is generally cloud free. Along these coasts, sea-breeze convergence is absent since the sea-breeze reinforces, rather than opposes, the light onshore wind. Similar cloud-free zones are seen over north-west facing coasts of Britain.

Infra-red data (not shown) indicated that all cloud tops terminated at low or middle levels, and reported precipitation was generally light, however, a waterspout was observed near Yarmouth, Isle of Wight.

Photograph by courtesy of University of Dundee

Meteorological Magazine

GUIDE TO AUTHORS

Content

Articles on all aspects of meteorology are welcomed, particularly those which describe the results of research in applied meteorology or the development of practical forecasting techniques.

Preparation and submission of articles

Articles for publication and all other communications for the Editor should be addressed to the Director-General, Meteorological Office, London Road, Bracknell, Berkshire RG12 2SZ and marked 'For *Meteorological Magazine*'.

Articles, which must be in English, should be typed, double-spaced with wide margins, on one side only of A4-size paper. Tables, references and figure captions should be typed separately.

Spelling should conform to the preferred spelling in the *Concise Oxford Dictionary*.

References should be made using the Harvard system (author, date) and full details should be given at the end of the text. If a document referred to is unpublished, details must be given of the library where it may be seen. Documents which are not available to enquirers must not be referred to.

Tables should be numbered using roman numerals and provided with headings. We consider vertical and horizontal rules to be unnecessary in a well-designed table; spaces should be used instead.

Mathematical notation should be written with extreme care. Particular care should be taken to differentiate between Greek letters and Roman letters for which they could be mistaken. Double subscripts and superscripts should be avoided, as they are difficult to typeset and difficult to read. Keep notation as simple as possible; this makes typesetting quicker and therefore cheaper, and reduces the possibility of error. Further guidance is given in BS1991: Part 1: 1976 and *Quantities, Units and Symbols* published by the Royal Society.

Illustrations

Diagrams must be supplied either drawn to professional standards or drawn clearly, preferably in ink. They should be about 1½ to 3 times the final printed size and should not contain any unnecessary or irrelevant details. Any symbols and lettering must be large enough to remain legible after reduction. Explanatory text should not appear on the diagram itself but in the caption. Captions should be typed on a separate sheet of paper and should, as far as possible, explain the meanings of the diagrams without the reader having to refer to the text.

Sharp monochrome photographs on glossy paper are preferred: colour prints are acceptable but the use of colour within the magazine is at the Editor's discretion. In either case contrast should be sufficient to ensure satisfactory reproduction.

Units

SI units, or units approved by WMO, should be used.

Copyright

Authors wishing to retain copyright for themselves or for their sponsors should inform the Editor when they submit contributions which will otherwise become UK Crown copyright by right of first publication.

It is the responsibility of authors to obtain clearance for any copyright material they wish to use before submitting it for publication.

Free copies

Three free copies of the magazine are provided for authors of articles published in it. Separate offprints for each article are not provided.

Meteorological Magazine

October 1987

Editor: R.W. Riddaway
Editorial Board: T. Davies, W.H. Moores, P.R.S. Salter, P.G. Wickham

Vol. 116
No. 1383

CONTENTS

Page

Case study of a persistent mesoscale cold pool. F.F. Hill and K.A. Browning 297

Variations in the onset of the summer monsoon over India. I. Subbaramayya, O.S.R.U. Bhanu Kumar and S. Vivekanandababu 309

Atmospheric research at the University of Manchester Institute of Science and Technology. C.P.R. Saunders 317

An appreciation of the work of Mr D.E. Miller. K.H. Stewart 324

Reviews

The elements of graphing data. W.S.Cleveland. *T.S. Hills* 326

Remote sensing digital image analysis. J.A. Richards. *C. Duncan* 326

Books received 327

Satellite photograph — 6 August 1987 at 1359 GMT 328

Contributions: it is requested that all communications to the Editor and books for review be addressed to the Director-General, Meteorological Office, London Road, Bracknell, Berkshire RG12 2SZ, and marked 'For *Meteorological Magazine*'. Contributors are asked to comply with the guidelines given in the *Guide to authors* which appears on the inside back cover. The responsibility for facts and opinions expressed in the signed articles and letters published in *Meteorological Magazine* rests with their respective authors. Authors wishing to retain copyright for themselves or for their sponsors should inform the Editor when submitting contributions which will otherwise become UK Crown copyright by right of first publication.

Subscriptions: Annual subscription £27.00 including postage; individual copies £2.30 including postage. Applications for postal subscriptions should be made to HMSO, PO Box 276, London SW8 5DT; subscription enquiries 01–211 8667.

Back numbers: Full-size reprints of Vols 1–75 (1866–1940) are available from Johnson Reprint Co. Ltd, 24–28 Oval Road, London NW1 7DX. Complete volumes of *Meteorological Magazine* commencing with volume 54 are available on microfilm from University Microfilms International, 18 Bedford Row, London WC1R 4EJ. Information on microfiche issues is available from Kraus Microfiche, Rte 100, Milwood, NY 10546, USA.

ISBN 0 11 727974 9

ISSN 0026–1149